APPLICATION OF LOW PLASTICITY BURNISHING (LPB) TO IMPROVE THE FATIGUE PERFORMANCE OF TI-6AL-4V FEMORAL HIP STEMS

D. Hornbach, Vice President Laboratory Operations, Lambda Technologies
P. Prevéy, President, Director of Research, Lambda Technologies
E. Loftus, Sr. Product Development Engineer, Exactech

ABSTRACT

Low plasticity burnishing (LPB) is a surface enhancement method that produces a deep layer of compressive residual stress with minimal cold working and an improved surface finish. Extensive fatigue testing, performed on numerous metal alloys in simulated environmental conditions, demonstrates that LPB significantly improves fatigue strength of highly stressed components. LPB is a flexible process, capable of being implemented on a wide variety of CNC machine tools.

A product-specific LPB process was developed and applied to the modular neck taper junction of a Ti-6Al-4V total hip prosthesis (THP). LPB produced a compressive residual stress field with an improved surface finish, which enhanced component fatigue strength and resistance to fretting damage. X-ray diffraction (XRD) residual stress measurements, made before and after LPB application, are shown. High cycle fatigue (HCF) results obtained on LPB-processed hip stems are shown along with baseline data for unprocessed hip stems. HCF tests demonstrate complete elimination of fretting fatigue failures in the LPB processed area of the taper junction and a substantial increase in overall THP fatigue strength.

KEYWORDS: Low Plasticity Burnishing (LPB), Total Hip Prosthesis, Residual Stress, High Cycle Fatigue (HCF), Surface Enhancement, Fretting Fatigue

INTRODUCTION

Total hip replacement surgery is often required to alleviate pain and improve the function of hips damaged from disease or fracture. It is estimated that over 300,000 hip replacement surgeries are performed each year in the United States alone. Implanted THP systems experience a spectrum of cyclic loading from normal day-to-day patient activities. Chances of HCF failure of the THP increase with patient size and level of activity.

Modular THP construction has become more widely used because it gives the surgeon the opportunity to interoperatively choose the proper size prosthesis and offers flexibility in treating a wide spectrum of hip defects and patient anatomies. Modular THP systems are typically held together using a tapered interlock. Fretting can occur along the contact of the taper junction due to small displacement between the two connected subcomponents. Surface micro-cracks from fretting damage can cause a significant reduction to the high cycle fatigue strength of the THP.

The benefits of compressive residual stresses to boost fatigue strength in metallic components have long been recognized.[1-4] Many engineering components have been cold worked using various surface enhancement processes such as shot peening to improve fatigue strength. A surface enhancement process termed low

plasticity burnishing (LPB) [5-9] has been shown to dramatically improve fatigue performance in components prone to damage such as foreign object damage (FOD),[10-12] fretting,[13-14] and pitting/corrosion.[15-18] LPB surface treatment is applied using conventional multi-axis CNC machine tools for unprecedented control of the residual stress distribution developed through modification of the pressure, feed, and tool characteristics. Achieving deep compression with low cold work reduces relaxation of the protective compressive layer either thermally during exposures at service temperatures[19], or mechanically due to overload or impact. In addition to the deep compressive residual stress produced, LPB dramatically improves the finish of most machined surfaces and in some cases leaves the surface with a near mirror finish.

During a continuous improvement assessment for the Exactech M-Series modular hip prosthesis, it was hypothesized that the controlled application of compressive residual stresses to the taper surface could improve fatigue strength without altering the prosthesis geometry. The possibility of keeping the same prosthesis geometry offered important advantages, including maintaining the existing size scope and utilization of existing inventory.

After experimentation with conventional roller burnishing and research into laser and shot peening, the LPB process was identified as the most promising surface treatment method for fatigue strength improvement in this application. An LPB process was designed to improve the fatigue strength and fretting damage tolerance of the M-Series modular hip prosthesis. A customized compressive residual stress field was developed for the tapered region of the neck stem segment using a detailed design protocol discussed in previous work [20]. Conventional roller burnishing was insufficient in terms of the compression produced and lacked the control required to produce consistent compressive residual stresses.

Experimental Method

Femoral Hip Stem Component

The Exactech M-Series Modular Hip Prosthesis is comprised of three major components that form a functional hip implant or prosthesis when assembled, as shown in Figure 1. These components include the femoral stem, metaphyseal and neck segments, and are held together with taper interfaces and a locking screw. In service, the neck segment taper experiences high-stress loading conditions in a corrosive, fretting environment. Furthermore, every step taken by a patient represents a single loading and unloading cycle that accumulates over years of implantation. Given this aggressive use environment, High Cycle Fatigue (HCF) strength is critical to the successful clinical performance of hip prostheses.

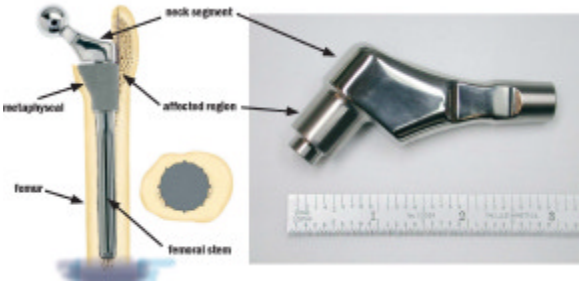

FIG. 1 - Exactech M-Series Modular Hip Prosthesis: Assembled Construct (left) and Neck Segment (right)

Baseline Fatigue Performance

To design the LPB zone it was first necessary to determine the fatigue initiation site. Several THP, with no LPB processing, were HCF tested to failure. Specifics of the HCF tests are discussed later.

Four hip stem segments, listed in Table 1, were examined optically at magnifications up to 60X and with a scanning electron microscope (SEM) to identify fatigue origins and locations thereof relative to the

specimen. Three of the four segments fractured in the tapered neck region. Specimen PR-2003-025-5 ran out to 10^7 cycles without failure to the neck.

TABLE 1 – Baseline hip stem segments used for fractography

Specimen	Load lbs (N)	Cycles to Failure
PR-2003-025-4	1500 (6672)	1,104,678
PR-2003-025-1	1800 (8007)	145,038
PR-2003-025-2	1200 (5338)	5,860,924
PR-2003-025-5	1050 (4671)	10,000,000 (Run-out)

Finite Element Modeling

Finite element (FE) modeling was used in the design of the compressive residual stress field of the hip stem. The model was used to estimate both the in-service applied stresses and the LPB residual stresses in the neck stem segment.

The 3-D model, shown in Figure 2, was composed of both the femoral neck stem segment and head. The neck segment and head were treated as one continuous body. The FE model consisted of 17334 first order brick elements and 6839 nodes. Typical solution treated and aged Ti-6Al-4V material properties were used.[21]

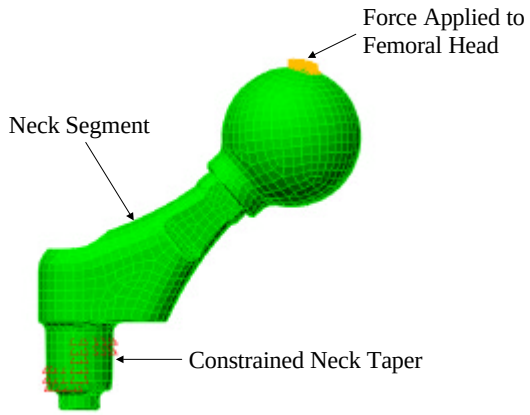

FIG. 2 – 3-D Finite element mesh for hip segment model.

Forces were placed on the femoral head to simulate the loads applied during fatigue testing. Applied stresses in the tapered neck region were determined for a 1050 and 1800 lb (4671 and 8007 N) load. The 1050 lb (4671 N) load was the fatigue strength of the THP with no LPB processing and the 1800 lb (8007 N) load was the fatigue strength target for an LPB processed neck segment. Nodal constraints were placed on the neck to simulate the boundary conditions between the tapered connection of the neck and the metaphyseal.

Residual stress results measured by XRD on LPB processed neck segments were placed in the FE model to accurately simulate the compression imparted by the LPB process. No attempt was made to model the plasticity that occurs during LPB since the exact residual stresses produced by LPB were measured by XRD. Compensatory tensile residual stresses around the compressive LPB zone were also estimated with the model.

LPB Processing

CNC control code was developed to allow positioning of the LPB tool in a series of passes around the stem neck taper in a CNC lathe. Burnishing loads were controlled to develop the desired magnitude of compressive stress with relatively low cold working. Figure 3 shows a stem neck segment being LPB processed in a four-axis manipulator on the CNC milling machine.

Residual Stress Characterization

XRD residual stress measurements were made employing a $\sin^2\psi$ technique and the diffraction of copper Ká1 radiation from the (21.3) planes, of the Ti-6Al-4V. It was first verified that the lattice spacing was a linear function of $\sin^2\psi$ æs required for the plane stress linear elastic residual stress model. [22-25]

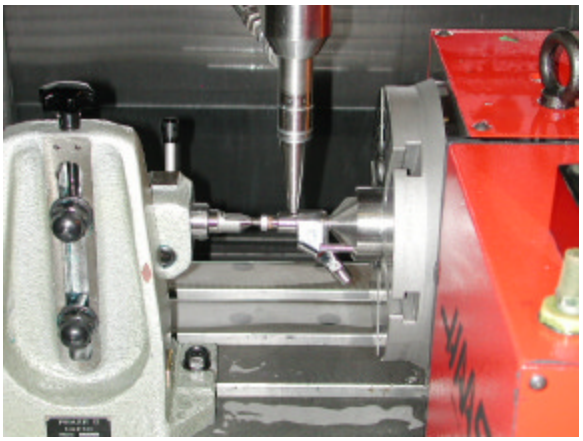

FIG. 3 - LPB processing of hip segment.

Material was removed electrolytically for subsurface measurement in order to minimize possible alteration of the subsurface residual stress distribution as a result of material removal. The residual stress measurements were corrected for both the penetration of the radiation into the subsurface stress gradient[26] and for stress relaxation caused by layer removal.[27]

The value of the x-ray elastic constants required to calculate the macroscopic residual stress from the strain normal to the (21.3) planes of the Ti-6Al-4V were determined in accordance with ASTM E1426-91.[28] Systematic errors were monitored per ASTM specification E915.

XRD residual stress measurements were made at the surface and at several depths below the surface on an as-received, roller burnished and LPB processed neck stem. Measurements were made on the processed o.d. of the neck to characterize the depth and magnitude of the compression produced. Measurements were also made on the i.d. bore of the neck to establish any change resulting from equilibrating tension. All measurements were made at mid-length of the neck taper, at the 12 o'clock position, as shown in Figure 4.

Residual stresses were measured at the 6 o'clock position, adjacent to the neck taper, on two neck segments following fatigue testing. Both neck segments ran out to 10^7 cycles at loads of 1400 lbs (6228 N) or greater. Measurements were made to ensure the LPB compressive residual stresses were not significantly altered. The applied compression at the 6 o'clock position is added to the compressive residual stresses from LPB, providing the potential for compressive yielding. Previous studies [29] have shown that compressive residual stresses can flip to tension after bulk yielding in either tension or compression. Residual stress inversion is more likely to occur in highly cold worked surfaces. Most machining and shot peening processes produce relatively high cold working compared to LPB.

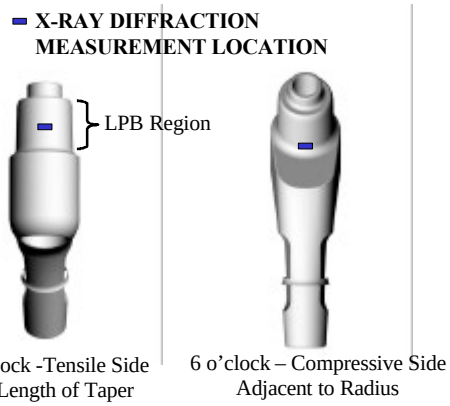

FIG. 4 - X-ray diffraction residual stress measurement locations.

Component Fatigue Testing

High cycle fatigue (HCF) testing performed on baseline and LPB processed neck segments were conducted on an MTS closed loop servo-hydraulic system in accordance with ISO standards 7206-4 and 7206-8.[30,31] A photo of the fatigue test setup is shown in Figure 5.

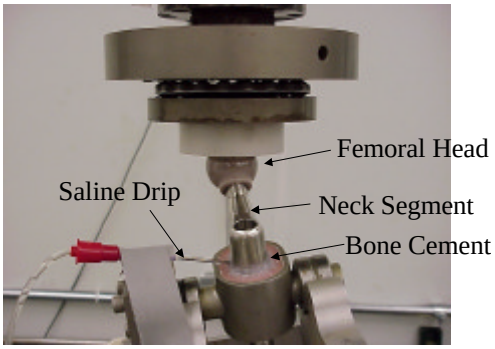

FIG. 5 - Fatigue test of THP system.

The metaphyseal and femoral stem were embedded in bone cement. A cyclic load was applied to the head producing bending and torsion about the processed neck region. A silicone bead was applied to seal the gap between the metaphyseal and the neck segment. A saline drip was introduced via needle injected into the silicone seal to maintain a wet saline environment at the modular taper junction.

Fatigue tests were run at an R of 0.1 and a frequency of 15 hertz. The systems were tested to failure, which was considered as a subcomponent breakage or loosening where the assembly is unable to support the applied loads. Specimen run-out was considered to be 10^7 cycles.

RESULTS AND DISCUSSION

Fractography

Figure 6 contains photographs of baseline Specimen PR-2003-025-2. Figure 6a shows the approximate location of the initiation site, which coincides with where finite element predicts the maximum tensile stress to occur. Fatigue cracks initiated on the outer diameter of the taper, near the 12 o'clock position. Multiple cracks in the hoop-radial plane are present at several positions along the length of the taper.

The micrograph in Figure 6b shows a magnified view of the failure. At higher magnification, it is apparent that the fatigue cracks initiated from fretting damage on the o.d.. Fretting damage resulted from relative motion between the tapered hip stem and the surrounding metaphyseal.

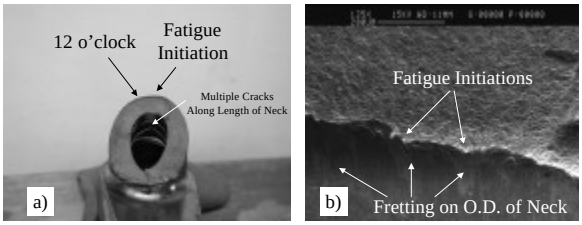

FIG. 6 – Optical a), and SEM micrograph b) of baseline Sample PR-2003-025-2 showing fretting fatigue initiations on o.d. adjacent to 12 o'clock position.

Specimens PR-2003-025-4 and PR-2003-025-1 failed at a similar location as PR-2003-025-2, near 12 o'clock on the o.d.. Both specimens failed from fretting damage that occurred on the o.d. of the neck. Both specimens contained multiple fatigue cracks at various positions along the neck length.

FIG. 7 – Optical photograph of metaphyseal used in conjunction with the testing of sample PR-2003-025-5. Note the cracking in the metaphyseal that occurred before complete failure of the construct.

Figure 7 shows a photograph of the metaphyseal from baseline Specimen PR-2003-025-5. The specimen was tested with a 1050 lb (4671 N) load for 10^7 cycles. While the neck taper did not catastrophically fail under this testing regime, further analysis revealed cracking in the metaphyseal.

Finite Element Modeling

Applied stress predictions from the FE model are shown in Figures 8a and 8b. Stresses are shown in the longitudinal direction relative to the neck taper axis, on both the o.d., and through the cross section of the taper region. Stresses are shown for an applied load of +1050 lbs (4671 N), which is the fatigue strength for the baseline condition. Peak tensile stresses on the order of +65 ksi (+448 MPa) are predicted on the o.d. The maximum applied stress is proximate to the 12 O'clock position due to the offset loading condition.

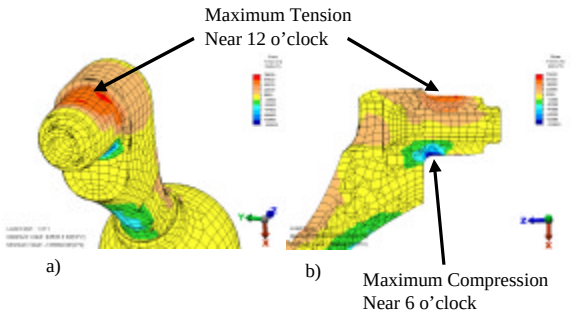

FIG. 8 -Finite element model showing the predicted applied stress resulting from a 1050 lb (4671 N) load on the o.d. a), and through the cross section b) of the neck segment taper.

Figures 9a and 9b show the residual stresses from LPB placed in the FE model on the o.d. and through the cross section of the taper, respectively. No residual tension is predicted at the surface of the taper region adjacent to the LPB processing. The LPB processed neck material pushes against the surrounding material resulting in compression in adjacent unprocessed areas. Subsurface compensatory tensile stresses on the order of +30 ksi (+207 MPa) or less were predicted below the compression from LPB. Tension on the i.d. bore increased +10 to +15 ksi (+69 to +103 MPa) as a result of introducing compression on the o.d.

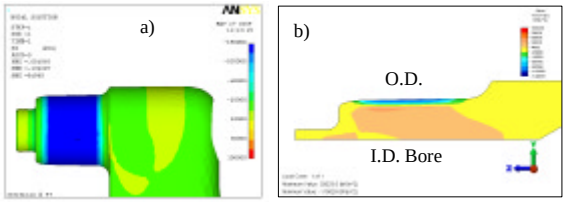

FIG. 9 - Compressive residual stresses imparted into femoral hip segment FE model. Residual stresses are shown on o.d. a), and through the cross section b).

Figure 10 shows the longitudinal applied stresses at 12 o'clock for both a 1050 and 1800 lb (4671 and 8007 N) load. Surface residual compressive stress measured by XRD on an LPB processed neck segment was added to the applied stress distributions to provide an estimate of the combined stress state. A horizontal line representing the fatigue strength of solution treated and aged (STA) Ti-6-4 [32] at 10^7 cycles, R=0 and Kt=1, is shown for comparison. Results indicate a maximum combined stress of close to +35 ksi (+241 MPa) on the o.d. at the start of the radius for the 1800 lb (8007 N) load. Combined stresses for the 1050 lb (4671 N) load was compressive throughout the taper region and less than half the fatigue strength of the 1800 lb (8007N) load. Results suggest that the neck stem should not fail in HCF in the LPB processed regions for loads up to at least 1800 lb (8007 N).

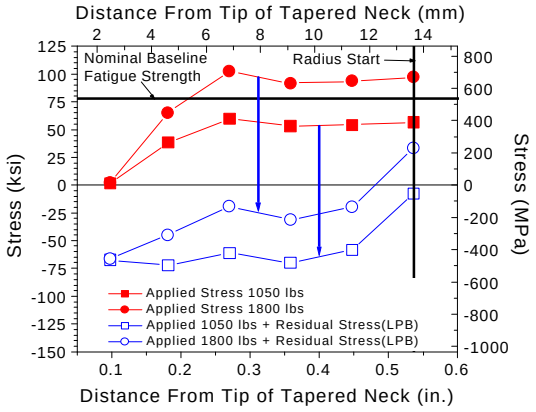

FIG.10 – Applied and combined (applied + residual stress) on o.d. of neck stem taper.

Residual Stress Measurements

The residual stress distributions measured by XRD on the o.d. of a baseline, roller burnished and LPB'ed hip segment are shown in Figure 11. A relatively shallow layer of compression exists on the hip stem in the baseline condition from the turning operation. Roller burnishing produced a depth of compression on the order of 0.02 in. (0.51 mm) with relatively low surface compression. LPB produced slightly greater than 0.03 in. (0.76 mm) depth of compression with near surface compression on the order of five times that produced by roller burnishing.

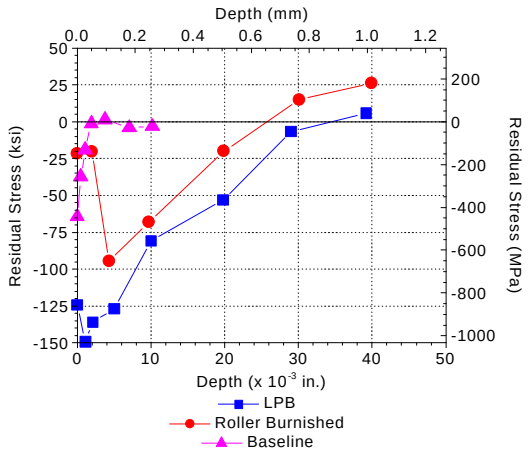

FIG. 11 – XRD residual stress vs. depth profiles on the o.d. of the tapered neck showing deeper and higher compression for LPB processed specimen.

XRD residual stresses measured at mid-length of the i.d. bore of the taper for the as-received, roller burnished and LPB'ed specimens were all compressive. All three samples had similar compression. As predicted by the FE model, the compensatory tension on the i.d. bore was negligible, and produced essentially no change to the residual stresses.

XRD residual stress results collected at the 6 o'clock position, adjacent to the radius, are shown in Figure 12. The applied compressive stresses from fatigue testing are not altering the compressive residual stresses significantly or causing a residual stress inversion from compression to tension.

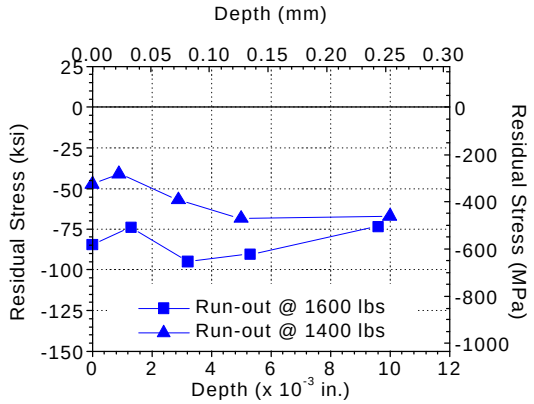

FIG. 12 - Residual stress vs. depth showing compression remaining on the compressively loaded side of the neck taper.

Fatigue Testing

Results for the HCF fatigue tests are presented graphically in Figure 13. The data are shown in a semi-log plot of maximum force vs. cycles to failure. Arrows indicate run-outs for both baseline and LPB'ed samples. Multiple run-outs were achieved for both sets of samples.

Baseline specimens were tested within a load range of 1050 to 1400 lbs (4671 to 6228 N). All fatigue failures in the baseline specimens occurred in the tapered neck region of the hip segment. Baseline results, shown in red symbols, indicate a fatigue strength at 10^7 cycles of 1050 lbs (4671 N).

LPB'ed neck segments were tested at loads of 1400 to 1600 lbs (6228 to 7117 N). LPB improved the fatigue strength of the hip stem greater than 40% and increased the life by over 10X as depicted by the blue symbols. The metaphyseal fractured on five of the LPB processed specimens ultimately ending the test. No failures initiated in the fretted LPB processed neck taper region. However, one failure occurred at 1500 lbs (6672 N) from fretting damage in the non-LPB'ed radius. Further refinement of the LPB process is

planned to include coverage of the radius, further strengthening the THP.

Additional HCF tests conducted on production neck segments confirm the fatigue strength of the neck segment to be at least 1400 lbs (6228 N). Future HCF tests are planned using larger metaphyseals to gage the true fatigue strength of the LPB'ed neck segment.

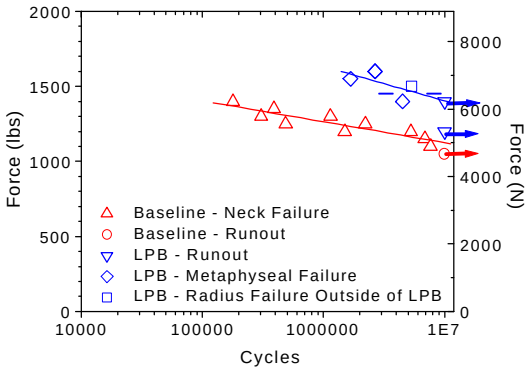

FIG. 13 - HCF results indicating LPB produces a nominal 40% increase in fatigue strength at 10^7 cycles. Arrows indicate run-outs at 10^7 cycles.

CONCLUSIONS

- LPB produced compressive residual stress in the stem neck segment to a depth of 0.03 in. (0.762 mm) with maximum compression approaching –150 ksi (-1034 MPa) near the surface. LPB produced a deeper layer of compression compared to roller burnishing with nominally 5X the compressive magnitude near the surface.

- LPB completely eliminated fretting failures in the processed neck stem region.

- LPB increased the fatigue strength of the THP by 40% above the baseline condition and increased the life by 10X. Fatigue cracks initiated in the metaphyseal in several of the LPB fatigue tests indicating the hip segment has a fatigue strength higher than 1400 lbs (6228 N). Further tests are being planned, with larger metaphyseals, to better determine the fatigue strength of the neck taper.

- Fractographic observations indicate that the prevalent location of failure initiation for baseline samples is approximately 30° to the clockwise of the 12 o'clock position (see figures for orientation). This trend in failure initiation location indicates that this position experiences high applied stress during loading as indicated from the finite element model. The baseline specimens generally have multiple initiations along the length of the taper which appear to be directly related to fretting damage occurring on the surface of the taper in the same general area.

ACKNOWLEDGEMENTS

The authors gratefully acknowledge Brian Tent, Doug Young, Chris Wahl and Tom Lachtrupp, from Lambda Technologies, for the fractography, finite element modeling, CNC code development, LPB design and residual stress measurement; and Robert Neugebauer and the staff at Martest Inc. for the HCF testing.

REFERENCES

[1] Frost, N.E. Marsh, K.J. Pook, L.P., *Metal Fatigue*, Oxford University Press, 1974.
[2] Fuchs, H.O. and Stephens, R.I., *Metal Fatigue In Engineering*, John Wiley & Sons, 1980.
[3] Berns, H. and Weber, L., "Influence of Residual Stresses on Crack Growth," Impact Surface Treatment, edited by S.A. Meguid, Elsevier, 33-44, 1984.
[4] Ferreira, J.A.M., Boorrego, L.F.P., and Costa, J.D.M., "Effects of Surface Treatments on the Fatigue of Notched Bend Specimens," Fatigue, Fract. Engng. Mater., Struct., Vol. 19 No.1, pp 111-117,1996.
[5] Prevéy, P.S. Telesman, J. Gabb, T. and Kantzos, P., "FOD Resistance and Fatigue Crack Arrest in Low Plasticity Burnished IN718", Proceedings of the 5th National HCF Conference, Chandler, AZ. March 7-9, 2000.

[6] U.S. Patents 5,826,453 (Oct. 1998), 6,415,486 B1 (Jul. 2002) other US and foreign patents pending.
[7] "Low Plasticity Burnishing", *NASA Tech Briefs*, Aug. 2002, pg. 50.
[8] "Longer Life with Low-Plasticity Burnishing", *Manufacturing Engineering*, SME, ed. Brian Hogan, Dec. 2001, pg. 34-38.
[9] T. Gabb, J. Telesman, P. Kantzos, P. Prevéy, "Surface Enhancement of Metallic Materials", *Advanced Materials & Processes*, ASM, ed. Peg Hunt, Jan. 2002, pg. 69-72.
[10] P. Prevéy, N. Jayaraman, R. Ravindranath, "Effect of Surface Treatments on HCF Performance and FOD Tolerance of a Ti-6Al-4V Vane," Proceedings 8th National Turbine Engine HCF Conference, Monterey, CA, April 14-16, 2003
[11] Paul S. Prevéy, Doug Hornbach, Terry Jacobs, and Ravi Ravindranath, "Improved Damage Tolerance in Titanium Alloy Fan Blades with Low Plasticity Burnishing," Proceedings of the ASM IFHTSE Conference, Columbus, OH, Oct. 7-10, 2002
[12] Paul S. Prevéy, et. al., "The Effect of Low Plasticity Burnishing (LPB) on the HCF Performance and FOD Resistance of Ti-6Al-4V," Proceedings: 6th National Turbine Engine HCF Conference, Jacksonville, FL, March 5-8, 2001.
[13] M. Shepard, P. Prevéy, N. Jayaraman, "Effect of Surface Treatments on Fretting Fatigue Performance of Ti-6Al-4V," Proceedings 8th National Turbine Engine HCF Conference, Monterey, CA, April 14-16, 2003
[14] Paul S. Prevéy and John T. Cammett, "Restoring Fatigue Performance of Corrosion Damaged AA7075-T6 and Fretting in 4340 Steel with Low Plasticity Burnishing," Proceedings 6th Joint FAA/DoD/NASA Aging Aircraft Conference, San Francisco, CA, Sept 16-19, 2002
[15] N. Jayaraman, Paul S. Prevéy, Murray Mahoney, "Fatigue Life Improvement of an Aluminum Alloy FSW with Low Plasticity Burnishing," Proceedings 132nd TMS Annual Meeting, San Diego, CA, Mar. 2-6, 2003.
[16] Paul S. Prevéy and John T. Cammett, "The Influence of Surface Enhancement by Low Plasticity Burnishing on the Corrosion Fatigue Performance of AA7075-T6," Proceedings 5th International Aircraft Corrosion Workshop, Solomons, Maryland, Aug. 20-23, 2002.
[17] John T. Cammett and Paul S. Prevéy, "Fatigue Strength Restoration in Corrosion Pitted 4340 Alloy Steel Via Low Plasticity Burnishing," Retrieved Sept. 2, 2003 from http://www.lambda-research.com/publica.htm.
[18] Paul S. Prevéy, "Low Cost Corrosion Damage Mitigation and Improved Fatigue Performance of Low Plasticity Burnished 7075-T6", Proceedings of the 4th Int. Aircraft Corrosion Workshop, Solomons, MD, Aug. 22-25, 2000.
[19] P. Prevéy, "The Effect of Cold Work on the Thermal Stability of Residual Compression in Surface Enhanced IN718", Proc. 20th ASM Materials Solutions Conf., St. Louis, MO, Oct. 10-12, 2000.
[20] Prevey, Paul S. and Jayaraman, N., "A Design Methodology to Take Credit for Residual Stresses in Fatigue Limited Designs," Journal of ASTM International, Vol.2, Issue 8, Sept., 2005, online.
[21] Alloy Digest, Filing Code Ti-66, July 1972, Engineering Alloys Digest, Inc.
[22] Hilley, M.E. ed.,(1971), Residual Stress Measurement by X-Ray Diffraction, *SAE HS-784*, (Warrendale, PA: Society of Auto. Eng.).
[23] Noyan, I.C. and Cohen, J.B., (1987) Residual Stress Measurement by Diffraction and Interpretation, (New York, NY: Springer-Verlag).
[24] Cullity, B.D., (1978) Elements of X-ray Diffraction, 2nd ed., (Reading, MA: Addison-Wesley), pp. 447-476.
[25] Prevéy, P.S., (1986), "X-Ray Diffraction Residual Stress Techniques," *Metals Handbook*, **10**, (Metals Park, OH: ASM), pp 380-392.
[26] Koistinen, D.P. and Marburger, R.E., (1964), Transactions of the ASM, **67**.
[27] Moore, M.G. and Evans, W.P., (1958) "Mathematical Correction for Stress in Removed Layers in X-Ray Diffraction Residual Stress Analysis," SAE Transactions, **66**, pp. 340-345
[28] Prevéy, P.S., (1977), "A Method of Determining Elastic Properties of Alloys in Selected Crystallographic Directions for X-Ray Diffraction Residual Stress Measurement," Adv. In X-Ray Analysis, **20**, (New York, NY: Plenum Press, 1977), pp 345-354.
[29] "The Effect of Prior Cold Working on the Development of Tensile Residual Stresses Following Bulk Deformation," Lambda Research - Diffraction Notes 28, Winter 2002
[30] "Determination of Endurance Properties of Stemmed Femoral Components with the Application of Torsion," ISO 7206-4; Geneva, Switzerland; 2002
[31] "Endurance Performance of Stemmed Femoral Components with Application of Torsion," ISO 7206-8; Geneva, Switzerland; 1995
[32] Aerospace Structural Metals Handbook, Book #4, Pg. 5, 1997 Edition.